Assessing Combinations of B(C6F5)3 and N2-Derived Molybdenum Nitrido Complexes for Heterolytic Bond Activation

Anaïs Coffinet, David Specklin, Quentin Le Dé, Soukaina Bennaamane, Luna Muñoz, Laure Vendier, Eric Clot, Nicolas Mézailles, Antoine Simonneau

Chemistry–A European Journal
Research Article
doi.org/10.1002/chem.202203774
Chemistry Europe
European Chemical Societies Publishing
www.chemeurj.org

Assessing Combinations of $B(C_6F_5)_3$ and N_2-Derived Molybdenum Nitrido Complexes for Heterolytic Bond Activation

Anaïs Coffinet[+],[a] David Specklin[+],[a] Quentin Le Dé,[a] Soukaina Bennaamane,[b] Luna Muñoz,[a] Laure Vendier,[a] Eric Clot,[c] Nicolas Mézailles,*[b] and Antoine Simonneau*[a]

Abstract: Two different dinitrogen-derived molybdenum nitrido complexes varying by their geometry, ligand spheres and oxidations states were shown to engage their N ligand in dative bonding with the strong Lewis acid $B(C_6F_5)_3$. The stable adducts were assessed for frustrated Lewis pair-type heterolytic E–H bond splitting of hydrosilanes (E = Si) and $HB(C_6F_5)_2$. Whereas Si–H bond activation was achieved, $HB(C_6F_5)_2$ was shown to substitute $B(C_6F_5)_3$ in a quantitative or equilibrated fashion, depending on the nature of the nitrido complex. No B–H bond splitting was observed. Thermodynamics of these reactions, computed by DFT, are in agreement with the experimental outcomes.

Introduction

Homogeneous catalytic formation of value-added compounds from dinitrogen other than ammonia, for which the Haber–Bosch process remains an unbeatable industrial supplier,[1] is a current and largely unmet challenge. Chemists have proposed rather mild solutions to make N_2 amenable to react with main group electrophiles, through its complexation to a metal center.[2] Such reactions have paved the way for the development of synthetic methods ultimately leading to (organo)nitrogen compounds and notably, the synthesis of silyl- or boryl-amines can be performed catalytically.[3,4] The finding of new catalyzed N_2 transformation processes mainly relies on the chemist's ability to make compatible as many elementary steps as possible within the proposed catalytic cycle; a common pitfall is indeed the coexistence, within the reaction mixture, of the strong reducing agents needed to generate a low valent metal species that activates dinitrogen and the electrophiles needed to functionalize it. This can be overtaken by achieving the reaction of mildly electrophilic compounds with dinitrogen complexes, for example hydrosilanes or hydroboranes. Our research groups have notably reported dinitrogen borylation methods using hydroboranes, employing either i) dinitrogen complexes or ii) a dinitrogen-derived Mo nitride.[5] In the first approach, the combination of a Lewis acidic borane in stoichiometric or catalytic amounts promotes the silylation or borylation of a dinitrogen ligand[6] under a mechanism reminiscent of the frustrated Lewis pair (FLP) chemistry.[7] In the second approach, a Mo(IV) nitride supported by a triphosphine ligand undergoes 1,2-B–H or -Si–H bond addition over the Mo–N linkage.[8] We hereby report results gathered while combining the two different approaches, that is, using combinations of N_2-derived nitrides with strong boron Lewis acids in order to promote mild N-functionalization in a FLP-type fashion. Comparable heterolytic bond cleavage reactions have been successfully implemented by the groups of Ison[9] and Mösch-Zanetti,[10] combining $B(C_6F_5)_3$ with metal oxo complexes (Figure 1),[11] while the team of Liddle has documented on H_2 splitting between a U(V) nitride (not derived from N_2) and $BMes_3$.[12]

Results and Discussion

We decided to study two different N_2-derived molybdenum nitrides, the seminal Mo(VI) nitrido complex (^{N}**MoN**) reported by Cummins and co-workers,[13] and the Mo(IV) congener (^{P}**MoN**) recently described by the team of Mézailles,[14] to verify whether the presence of d electrons could have an impact in this reactivity context. We commenced our investigations by checking the stability of ^{N}**MoN** and ^{P}**MoN** with the strong Lewis

[a] Dr. A. Coffinet,[+] Dr. D. Specklin,[+] Q. Le Dé, L. Muñoz, Dr. L. Vendier, Dr. A. Simonneau
LCC-CNRS
Université de Toulouse, CNRS, UPS
205 route de Narbonne, BP44099, F-31077 Toulouse cedex 4 (France)
E-mail: antoine.simonneau@lcc-toulouse.fr
Homepage: https://www.lcc-toulouse.fr/activation-de-petites-molecules-equipe-n/
[b] Dr. S. Bennaamane, Dr. N. Mézailles
Laboratoire Hétérochimie Fondamentale et Appliquée
Université Paul Sabatier, CNRS
118 Route de Narbonne, 31062 Toulouse (France)
E-mail: mezailles@chimie.ups-tlse.fr
Homepage: https://lhfa.cnrs.fr/index.php/equipes/shen
[c] Dr. E. Clot
ICGM, Univ. Montpellier, CNRS, ENSCM
34000 Montpellier (France)

[+] These authors contributed equally to this manuscript.

Supporting information for this article is available on the WWW under https://doi.org/10.1002/chem.202203774

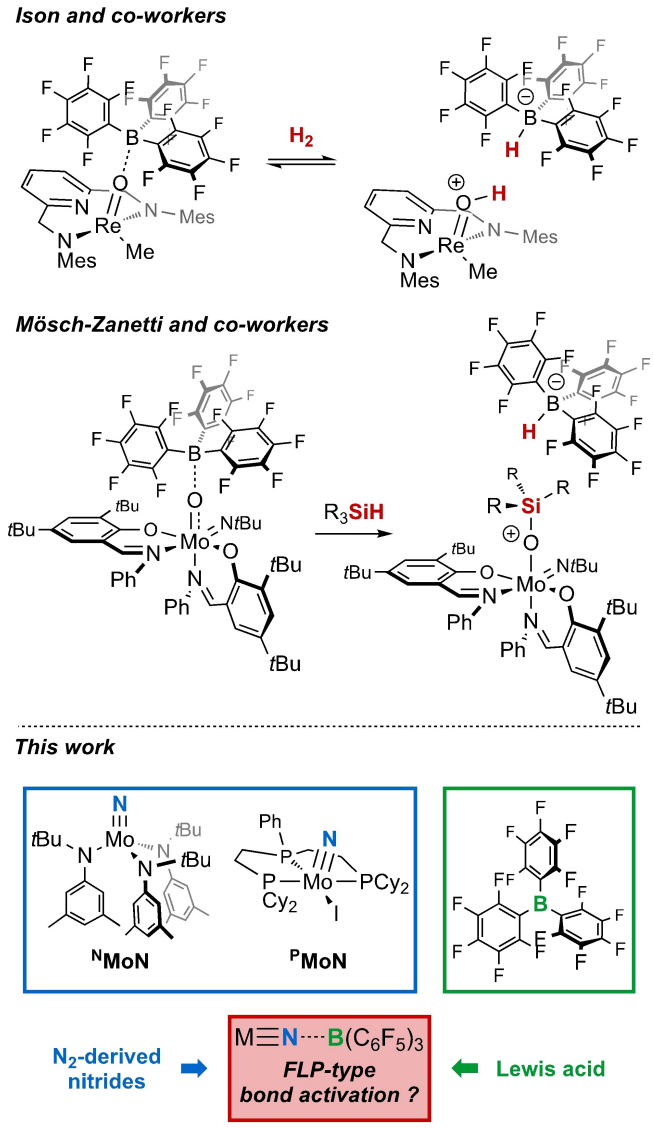

Figure 1. FLP-related heterolytic bond cleavage employing transition-metal oxos as the Lewis base component (top) and overview of the present work: exploring N_2-derived nitrides and $B(C_6F_5)_3$ combinations for FLP-type bond activation.

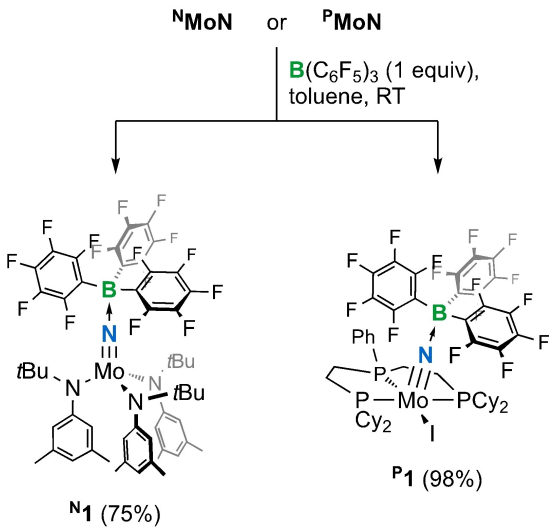

Scheme 1. Formation of Lewis acid-base adducts ^{N}**1** and ^{P}**1** between Mo nitrides and $B(C_6F_5)_3$.

acid (LA) $B(C_6F_5)_3$. Treating solutions thereof in either deuterated benzene or toluene with an equimolar amount of $B(C_6F_5)_3$ at room temperature immediately led to the quantitative formation of the new compounds ^{N}**1** and ^{P}**1** according to NMR (^{1}H, ^{11}B, ^{19}F and ^{31}P) analysis (Scheme 1). For both Mo compounds, the boron resonance of $B(C_6F_5)_3$ in the ^{11}B NMR spectra was strongly shifted to higher fields, from 58 to 4 and −5 ppm when complexed to ^{N}**MoN** and ^{P}**MoN**, respectively. The expected superior electron richness of the nitrogen atom in ^{P}**MoN** due to the presence of d electrons can be correlated to the stronger shielding of the boron atom in ^{P}**1**. ^{1}H and ^{31}P NMR spectra did not suggest important changes in the coordination spheres of the metal centers, although interaction with the boron LA indeed impacted chemical shifts of the proton and phosphorus resonances. These data indicated quite unambiguously that the boron LA is complexed to the nitrido ligand, and are unsurprising: an exhaustive study of LA complexation to ^{N}**MoN** was already performed by Cummins and his team (with exclusion of $B(C_6F_5)_3$),[15] whereas the Schrock group reported a stable adduct of $B(C_6F_5)_3$ with an N_2-derived Mo(VI) nitride.[16] Besides, several stable $B(C_6F_5)_3$ adducts of nitrido complexes are found in the literature.[17] We succeeded in obtaining a solid-state structure for ^{N}**1** (Figure 2). Selected geometric parameters can be found in Table 1. The compound exhibits C_{3v} symmetry,

Table 1. Selected bond lengths (Å) and angles (°) for the compounds prepared in this study as well as related ones. L represents any atom of the ancillary ligand (nitrogen or phosphorus) attached to the metal center. E = B or Si. R = C_6F_5, F, Me, Ph or H. n.a. = not applicable.

Distance/Angle	^{N}MoN[a]	^{P}MoN[b]	^{N}1	^{N}MoN···BF_3[c]	^{N}2b	[^{N}MoNSiMe$_3$]$^{+}$[c]	^{N}3
Mo–N	1.651(4)	1.656(2)	1.727(1)	1.678(4)	1.729(5)	1.716(3)	1.712(2)
Mo–L	1.964(4)[d]	2.4895(8)[e]; 2.4051(8)[f]	1.968(1)[d]	1.944(1)[d]	1.953(2)[d]	1.936(0)[d]	1.960(6)[d]
N–E	n.a.	n.a.	1.627(2)	1.609(7)	1.796(5)	1.795(4)	1.587(3)
Mo–N–E	n.a.	n.a.	179.4(1)	177.6(4)	178.8(3)	180.0(2)	169.8(1)
N–Mo–L[d]	103.4(2)	100.9(1)[g]; 105.0(1)[h];	110.2(1)	105.5(8)	108.8(6)	108.1(0)	107.2(8)
N–E–R[d]	n.a.	n.a.	108.9(1)	107.7(3)	108.0(3)	107.6(0)	109(6)

[a] taken from Ref. [13b]. [b] taken from Ref. [14]. [c] taken from Ref. [15]. [d] averaged data, standard deviation calculated from the measurement set and are not the average of the standard deviation of individual measurements. [e] average Mo-PCy_2 bond length. [f] Mo-PPh bond length. [g] averaged N–Mo-PCy_2 angle. [h] N–Mo-PPh.

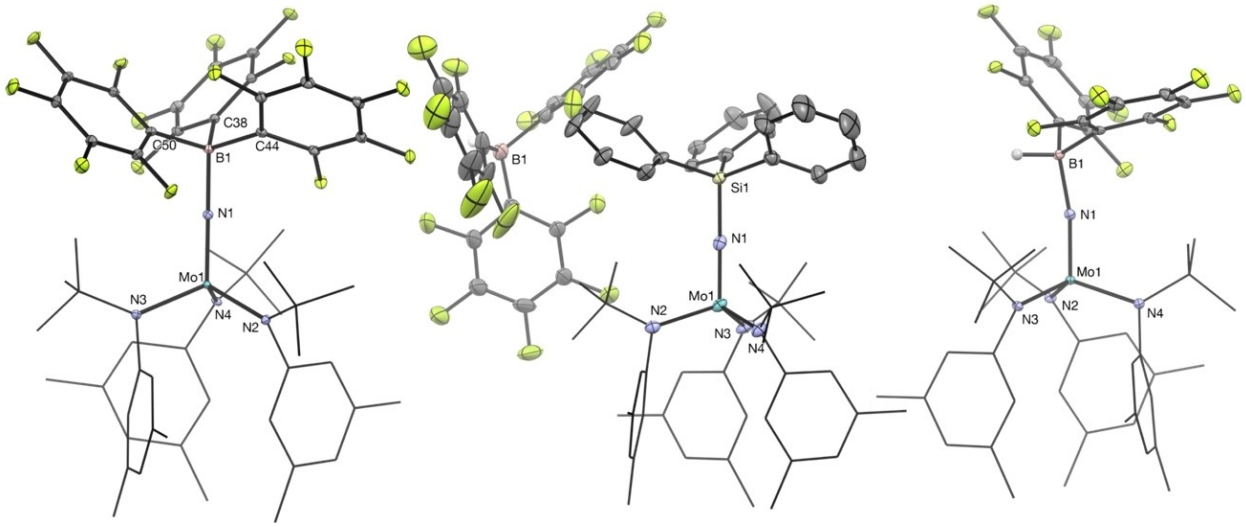

Figure 2. Solid-state molecular structures of, from left to right, ^{N}**1**, ^{N}**2b** and ^{N}**3**. Ellipsoids are drawn at the 30% probability level. Substituents of the anilide ligands are depicted as wireframes and all hydrogen atoms except those bound to boron are omitted for clarity.

with boron's substituents eclipsed with the anilide ligands. Both Mo and B atoms are in an almost perfect tetrahedral geometry and the Mo-N–B arrangement is linear. Compared to ^{N}**MoN**, the nitride Mo≡N bond in ^{N}**1** is longer (+0.08 Å). Similar elongation was recorded upon complexation of $B(C_6F_5)_3$ with a Mo(VI) nitride[16] and likely results from the substitution of the N atom giving the Mo–N linkage more imido character. The other Mo–N distances are not significantly changed, but the steric repulsion from the C_6F_5 groups pushes the anilide ligands away (average N–Mo–N angles wider by 7°). It is worth comparing the structure of ^{N}**1** with the BF_3 adduct of ^{N}**MoN**.[15] In the latter, the B and Mo substituents adopt a staggered conformation. This difference probably arises from Van der Waals interaction between the *t*Bu hydrogens and the fluorine atoms. Shorter Mo–N and N–B bond lengths are also recorded, presumably as the result of diminished sterics and electrophilicity[18] of the BF_3 fragment compared to $B(C_6F_5)_3$.

Having established the stability of the two $B(C_6F_5)_3$-complexed nitrido compounds, we next embarked on the study of their reactivity towards the heterolytic splitting of Si–H bonds.[19] Compounds ^{N}**1** and ^{P}**1** were next reacted with the hydrosilane Et_3SiH. Clean formation of the new compounds ^{N}**2a** and ^{P}**2a** were readily observed at room temperature, within 10 min and 18 h, respectively (Scheme 2). NMR analyses were in agreement with the heterolytic cleavage of the Si–H bond between the nitrido complex and $B(C_6F_5)_3$: the Si–H resonance in ^{1}H NMR disappeared, while ^{11}B and ^{19}F NMR spectra clearly indicated the formation of the $[HB(C_6F_5)_3]^-$ anion. For ^{P}**2a**, the two ^{31}P resonances were deshielded compared to ^{P}**1**. Longer reaction time in the case of ^{P}**1** could be attributed to the shielding provided by the bulky cyclohexyl groups of the phosphines. Neither ^{N}**1** nor ^{P}**1** were reactive towards Et_3SiH in the absence of $B(C_6F_5)_3$ under the same conditions.

We were not able to grow single crystals of these new compounds due to their tendency to give oily precipitates, but

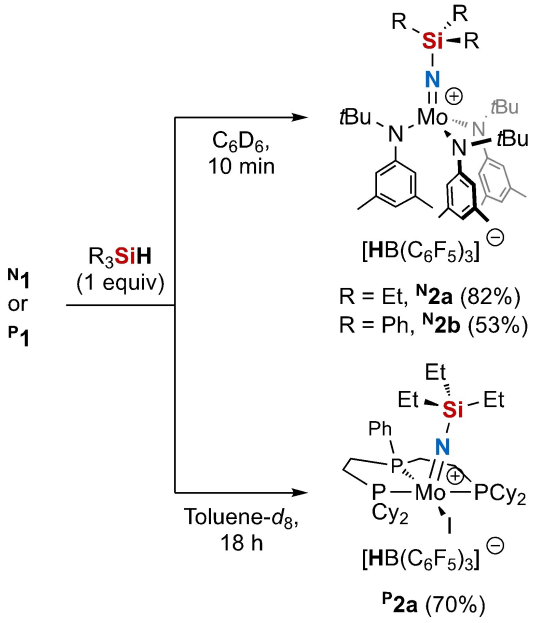

Scheme 2. Si–H bond splitting by $B(C_6F_5)_3$ / Mo nitride Lewis pairs.

the phenyl analog ^{N}**2b**, obtained from the reaction of ^{N}**1** with Ph_3SiH (Scheme 2), gave after recrystallization material suitable for a single-crystal X-ray diffraction (sc-XRD) analysis (Figure 2). This allowed us to confirm the splitting of the Si–H bond, resulting in the silylation of the nitrido ligand to form a cationic silylamido-Mo species. The C_3-symmetric structure of ^{N}**2b** closely resembles the one of the silylimido-Mo complex obtained after treatment of ^{N}**MoN** with Me_3SiOTf (Table 1).[15] The silicon substituents are not completely eclipsed with the anilide ligands. Expectedly, the Mo–N–Si array is linear, with Mo–N and N–Si bonds 1.729(5) and 1.796(5) Å long, respectively.

We next turned our attention towards B–H bond activation.[20] Aside from ligand sphere and oxidation state, a striking difference between ^{N}**MoN** and ^{P}**MoN** is that the first is unreactive towards hydroboranes (HBR_2) while the second readily undergoes 1,2-B–H bond addition of pinacol borane (HBpin) over the Mo–N linkage.[8b] We have also demonstrated that for zerovalent diphosphine-supported group 6 dinitrogen complexes, Piers' borane ($HB(C_6F_5)_2$) can assist 1,3-B–H bond addition over the M–N≡N unit.[6b,c] These previous results pushed us to treat ^{N}**MoN** and ^{P}**MoN** with $HB(C_6F_5)_2$ to verify whether the nitrido species undergo similar reactivity with this borane. Both ^{N}**MoN** and ^{P}**MoN** reacted cleanly with $HB(C_6F_5)_2$ to give the new compounds ^{N}**3** and ^{P}**3** exhibiting comparable spectroscopic signatures to ^{N}**1** and ^{P}**1** (Scheme 3). Notably, the absence of a hydride signal in the ^{1}H NMR spectra of either ^{N}**3** or ^{P}**3** was a clear indication that 1,2-B–H bond addition did not occur, simple Lewis acid-base adducts being formed instead, showing no evolution upon heating (90 °C). While this is not a surprise in the case of ^{N}**MoN**, it could have been expected that Piers' borane adds over the Mo–N bond of ^{P}**MoN**. We believe that electronic and steric factors explain this discrepancy, since $HB(C_6F_5)_2$ is a weaker hydride donor[21,22] and bears higher steric penalty than HBpin due to its bulky C_6F_5 groups. We were able to perform an sc-XRD analysis of ^{N}**3** (Figure 2), confirming adduct formation between Piers' borane and ^{N}**MoN**. Structural comparison of ^{N}**1** and ^{N}**3** reveals some differences regarding the Mo-N–B arrangement: in the latter, it deviates quite significantly from linearity (170 vs. 179°), allowing the C_6F_5 groups to be pushed away from the *t*Bu substituents of the anilide ligands and thus diminishing steric repulsion. While Mo–N distances are similar in ^{N}**1** and ^{N}**3**, the N–B bond is shorter in the latter (1.587(3) vs. 1.627(2) Å), being comparable to the one found in the BF_3 adduct (1.609(7) Å, see Table 1). The diminished steric repulsion resulting from the replacement of a C_6F_5 group by H likely explains this difference. Attempts to perform B–H bond activation/B-to-B hydride transfer with $B(C_6F_5)_3$ in ^{N}**3** and ^{P}**3** to form cationic borylimido complexes were not successful: addition of one equivalent to a solution of ^{N}**3** resulted in no reaction, while in the case of ^{P}**3**, a ca. 50:50 mixture of ^{P}**1** and ^{P}**3** was obtained (see Supporting Information section II.7.9). The preference of ^{N}**MoN** to preferably pair with $HB(C_6F_5)_2$ over $B(C_6F_5)_3$) was confirmed by treating ^{N}**1** with one equivalent of Piers' borane, affording ^{N}**3** selectively (Scheme 3).

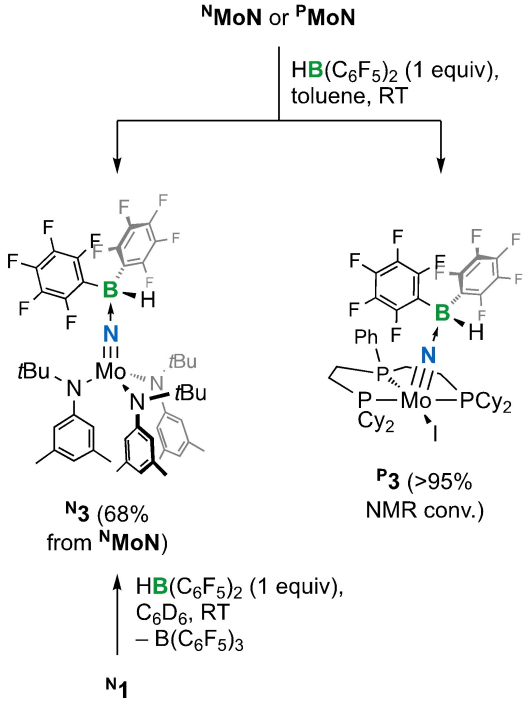

Scheme 3. Reactivity of Piers' borane with nitride complexes ^{N}**MoN** and ^{P}**MoN**, and $B(C_6F_5)_3$-adduct ^{N}**1**.

It could have been expected that the higher steric shielding around ^{P}**MoN**'s nitrido moiety would have favoured its association with $HB(C_6F_5)_2$. We indeed suggested this property to explain the difference in rates for the silylation of the two studied species (see above). We propose that steric shielding may facilitate borane dissociation, leading to a seemingly equilibrated mixture of ^{P}**1** and ^{P}**3** when the latter was reacted with $B(C_6F_5)_3$ – its square-pyramidal ligand environment may not help discriminate significantly between the two planar tricoordinated boranes, as opposed to C_{3v}-symmetric ^{N}**MoN**. It can well be that, in the Si–H bond activation reaction (Scheme 2), the rate-limiting step is actually the N–Si bond formation following nucleophilic attack of the nitride onto the $B(C_6F_5)_3$-activated silane.[23] It would be therefore kinetically disfavoured in the case of ^{P}**MoN**.

To rationalize the reactivity, or lack thereof, of the nitride complexes toward the boranes and triphenylsilane, DFT (PBE0-D3) calculations have been carried out on the actual experimental systems (see Scheme 4 and the Supporting Information for the computational details). Solvent effects were taken into account via the SMD model (benzene). We limited our study to the complexes of Mo(VI) as X-ray data was available for direct comparison with DFT optimized structures. First, the borane adducts were computed. The adduct with Piers' borane, ^{N}**3**, was computed $\triangle G = -18.0$ kcal mol^{-1} more stable than the separated reagents ^{N}**MoN** and $HB(C_6F_5)_2$, while the one with $B(C_6F_5)_3$, ^{N}**1**, was computed to be in equilibrium ($\Delta G = 0.4$ kcal mol^{-1}). This is essentially due to entropic effects as the energy only difference $\Delta E = -25.7$ kcal mol^{-1}, attests a favorable N→B interaction with $B(C_6F_5)_3$ although being rather weak. Interestingly, the borane exchange reaction that forms ^{N}**3** ($HB(C_6F_5)_2$ adduct) from ^{N}**1** ($B(C_6F_5)_3$ adduct) was computed to be exoergic by $\triangle G = 18.4$ kcal mol^{-1}, in accord with experiments demonstrating fast and quantitative $B(C_6F_5)_3$ displacement by $HB(C_6F_5)_2$. We next computed the activation of Ph_3SiH by ^{N}**MoN** and $B(C_6F_5)_3$. The separated charged species $[^{N}$**MoN**$SiPh_3]^+$ and $[HB(C_6F_5)_3]^-$ were optimized, and even in that case, the reaction was computed to be exergonic ($\triangle G = -1.4$ kcal mol^{-1}). The associated ion pair, $[^{N}$**MoN**$SiPh_3]^+[HB(C_6F_5)_3]^-$ (i.e., ^{N}**2b**) was then optimized, which resulted in a significant stabilization of $\triangle G = -3.9$ kcal mol^{-1} with respect to the separated ions. Overall, the formation of ^{N}**2b** from ^{N}**MoN**, $B(C_6F_5)_3$ and Ph_3SiH is exergonic by $\triangle G = -5.3$ kcal mol^{-1}, and thus consistent with experimental observations. Finally, boron-to-boron hydride

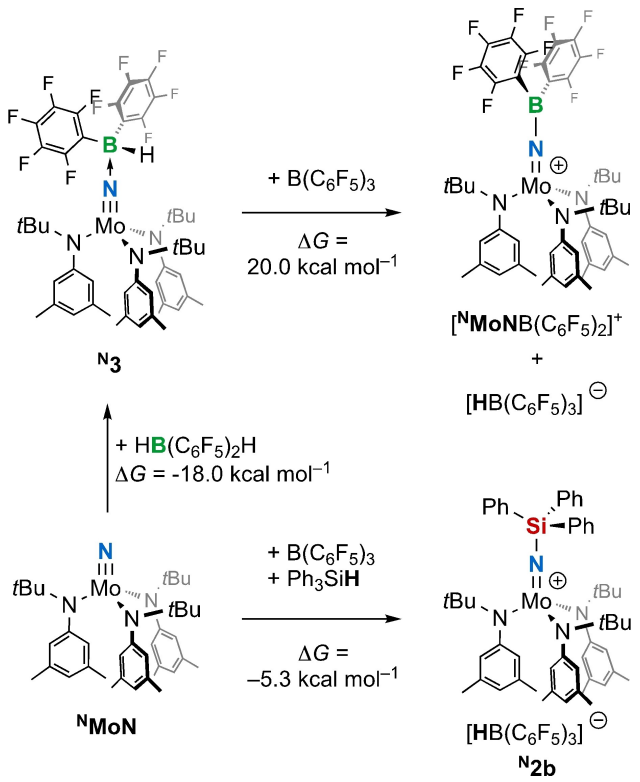

Scheme 4. Gibbs free energies calculated by DFT (PBE0-D3) for the experimentally verified formation of ^{N}**2b** and ^{N}**3** as well as B–H bond activation leading to the hypothetical species $[^{N}\mathbf{MoN}B(C_6F_5)_2]^+$.

transfer from ^{N}**3** to $B(C_6F_5)_3$ was computed to be endoergic by $\Delta G = 20.0$ kcal mol^{-1} when formation of the separated products $[^{N}\mathbf{MoN}B(C_6F_5)_2]^+$ and $[HB(C_6F_5)_3]^-$ was considered. Attempts to locate an associated ion pair on the potential energy surface failed as geometry optimization could not reach convergence. However, the significant endoergic character of the B–H bond activation process speaks against any experimental observation of such a transformation, in agreement with our experimental observation.

Conclusion

In this article, we have assessed the ability of N_2-derived nitrides ^{N}**MoN** and ^{P}**MoN** to act as the Lewis base component of an FLP system for Si–H and B–H bond cleavage. While both species were shown to be competent for Si–H bond activation of tertiary silanes, affording cationic silylimido species ^{N}**2** and ^{P}**2**, B–H bond activation of Piers' borane could not be achieved, stable Lewis acid-base adducts ^{N}**3** and ^{P}**3** being formed instead. Computed Gibbs free energies of these reactions in the case of ^{N}**MoN** were found consistent with the observed reactivity or lack thereof. Unlike previously described with other hydroboranes,[8] ^{P}**MoN** did not undergo 1,2-B–H bond addition over the Mo–N linkage. Structural data could be collected from crystalline materials obtained from the reactions involving ^{N}**MoN**, allowing for a comparison between the new species as well as with previously reported ones. These results encourage us to investigate the FLP-type activation of other substrates, such as olefins, CO_2, or H_2.

Experimental Section

General information: All reactions were performed in flame- or oven-dried glassware with rigorous exclusion of air and moisture, using a nitrogen- or argon-filled Jacomex glove box ($O_2 < 1$ ppm, $H_2O < 1$ ppm) equipped with a vacuum line. Solvents used were pre-dried (toluene, tetrahydrofuran, dichloromethane, diethyl ether and *n*-pentane by passing through a Puresolv MD 7 solvent purification machine; *n*-hexane and hexamethyldisiloxane (HMDSO) by distillation over CaH_2), degassed by freeze-pump-thaw cycles, dried over molecular sieves and stored in the glove box. C_6D_6, toluene-d_8 and PhCl-d_5 (purchased from Eurisotop) were degassed by freeze-pump-thaw cycles, dried over molecular sieves and stored in the glove box. [Mo(N){N(*t*Bu)(*m*-xyl)}$_3$] (^{N}**MoN**),[24] [MoI(N)-{PhP($CH_2CH_2PCy_2$)$_2$}] (^{P}**MoN**),[14] $B(C_6F_5)_3$,[25] and $HB(C_6F_5)_2$[26] were synthesized according to reported procedures and stored in the glove box. Triethylsilane and triphenylsilane were purchased from Sigma-Aldrich; the former was distilled over CaH_2, degassed and stored in the glove box; the latter was used as received. ^{1}H, ^{11}B, ^{19}F, ^{15}N and ^{31}P NMR spectra were recorded in C_6D_6, toluene-d_8 or PhCl-d_5 on a Bruker Avance III 400 spectrometer. Chemical shifts are in parts per million (ppm) downfield from tetramethylsilane and are referenced to the residual solvent resonances as the internal standard. ^{11}B, ^{19}F, ^{29}Si and ^{31}P NMR spectra were calibrated according to the IUPAC recommendation using a unified chemical shift scale based on the proton resonance of tetramethylsilane as primary reference.[27] Data are reported as follows: chemical shift, multiplicity (br = broad, s = singlet, d = doublet, t = triplet, q = quartet, p = quintet, m = multiplet), coupling constant (Hz), and integration. Infrared (IR) spectra were recorded in the glove box on an Agilent Cary 630 FTIR spectrophotometer equipped with ATR or transmission modules and are reported in wavenumbers (cm^{-1}) with (s) and (m) indicating strong and medium absorption, respectively. Elemental analyses were performed on samples sealed in tin capsules under N_2 by the Analytical Service of the Laboratoire de Chimie de Coordination; results are the average of two independent measurements.

Synthesis and characterization of ^{N}1: In the glove box, [Mo(N){N-(*t*Bu)(*m*-xyl)}$_3$] (^{N}**MoN**, 38.4 mg, 60.0 µmol, 1.00 equiv.) and $B(C_6F_5)_3$ (30.8 mg, 60.0 µmol, 1.00 equiv.) were introduced into a flask and dissolved in 1.5 mL of toluene. The reaction was immediate. Pentane (8 mL) was added to the yellow solution. Some insoluble, colorless material was removed by filtration and the filtrate was concentrated to 5–6 mL. The solution is then stored in the freezer of the glove box (−35 °C) for one week. During this time, yellow crystals of ^{N}**1** formed (52.2 mg, 45.3 µmol, 75 %). ^{1}H NMR (400 MHz, C_6D_6) δ 6.70 (s, 3H), 5.61 (s, 6H), 2.05 (s, 18H), 1.12 (s, 27H). ^{11}B NMR (128 MHz, C_6D_6) δ 3.9. ^{19}F NMR (377 MHz, C_6D_6) δ −115.2–−138.6 (br s, 6F), −156.1 (br s, 3F), −162.9 (s, 6F). IR (ATR) ν = 2978, 2930, 1645, 1600, 1584, 1517, 1450, 1393, 1377, 1365, 1359, 1280, 1163, 1141, 1095, 1041, 1009, 981, 971, 944, 925, 897, 888, 852, 840, 781, 773, 736, 714, 689, 675. Elem. Anal. calcd. for $C_{54}H_{54}BF_{15}MoN_4$: C 56.36; H 4.73; N 4.87. Found: C 56.77; H 4.68; N 4.79.

Synthesis and characterization of ^{P}1: In a glove box, [MoI(N)-{PhP($CH_2CH_2PCy_2$)$_2$}] (^{P}**MoN**, 10 mg, 12.5 µmol, 1.0 equiv.) was weighed in a screw-cap 4-mL vial. After addition of a magnetic stir bar, the solid was layered with a toluene-d_8 solution (0.5 mL) of $B(C_6F_5)_3$ (6.4 mg, 12.5 µmol, 1.0 equiv.). The vial was capped and stirred for a few minutes. The resulting dark-red solution was transferred to a J-Young NMR tube. The reaction vial was washed

with 0.1 mL of toluene-d_8 and the wash was added to the NMR tube. NMR analysis confirmed the formation of ^{P}**1** in a >95% spectroscopic yield. Back to the glove box, the solution was transferred to a round-bottom 10-mL screw-cap tube and concentrated to dryness. The residue was then triturated in a few milliliters of pentane to give 16.3 mg of an amorphous solid (98% yield). ^{1}H{^{31}P} NMR (400 MHz, Toluene-d_8) δ 7.61 (d, J=7.7, 2H), 7.31 (t, J=7.6, 2H), 7.21 (t, J=7.4, 1H), 2.54 (t, J=10.9, 2H), 2.45 (d, J=12.2, 2H), 2.29–2.18 (m, 4H), 2.11–2.03 (m, 2H), 1.87–1.73 (m, 6H), 1.67–1.55 (m, 6H), 1.55–1.39 (m, 4H), 1.38–1.07 (m, 12H), 1.06–0.77 (m, 12H), 0.73 (d, J=11.0, 2H). ^{11}B NMR (128 MHz, Toluene-d_8) δ −5.0. ^{19}F NMR (377 MHz, Toluene-d_8) δ −129.1 (d, J=23.1, 6F), −160.6 (t, J=20.8, 3F), −165.4 (t, J=20.0, 6F). ^{31}P{^{1}H} NMR (162 MHz, Toluene-d_8) δ 93.0 (1P), 60.6 (2P). IR (ATR) ν=2923, 2849, 1642, 1513, 1460, 1446, 1276, 1082, 975, 886, 852, 788, 729. Elem. Anal. calcd for $C_{34}H_{57}IMoNP_3$: C, 51.33; H, 7.22; N, 1.76. Found: C, 51.75; H, 6.98; N, 1.68.

Synthesis and characterization of ^{N}2a: In the glove box, [Mo(N){N(*t*Bu)(*m*-xyl)}$_3$] (^{N}**MoN**, 19.2 mg, 30.0 μmol, 1.00 equiv.) and B(C_6F_5)$_3$ (15.4 mg, 30.0 μmol, 1.00 equiv.) were weighed in a screw-cap 4-mL vial. A magnetic stir bar was placed in the vial and 0.6 mL of C_6D_6 was added. After 5 min. of stirring, the clear yellow solution was transferred to a J-Young NMR tube. NMR analysis revealed the complete formation of ^{N}**1** in a >95% spectroscopic yield. Back to the glove box, the C_6D_6 solution was transferred to the reaction vial, and triethylsilane (4.8 μL, 30 μmol, 1.0 equiv.) was added using a Hamilton® micro-syringe. After 5 min., a brown oil started to precipitate. Pentane (2 mL) was added, causing the precipitation of more brown oil. The supernatant was discarded, and the oil was washed twice with pentane (ca. 2 mL). The residue was dried under vacuum, then taken up again in pentane and triturated until the oil became a yellow powder. After discarding the liquid phase and drying under vacuum, solid ^{N}2a weighed 31 mg (82% yield). ^{1}H NMR (400 MHz, PhCl-d_5) δ 7.20-5.60 (br s, 6H), 6.78 (s, 3H), 4.45 (q, J_{HB}=77.0, 1H), 2.05 (s, 18H), 1.10 (s, 15H), 1.06 (s, 27H). ^{11}B NMR (128 MHz, PhCl-d_5) δ −24.6 (d, J_{BH}=67.6). ^{19}F NMR (377 MHz, PhCl-d_5) δ −132.3 (d, J=21.7), −164.3 (t, J=20.6), −166.8 (td, J=23.8, 6.8). ^{1}H-^{29}Si HMQC NMR (400, 80 MHz, PhCl-d_5) δ −29.8. IR (ATR) ν=2981, 2934, 2401, 1638, 1601, 1584, 1506, 1457, 1391, 1378, 1364, 1272, 1244, 1164, 1144, 1114, 1100, 1073, 1005, 964, 947, 896, 760, 743, 711, 691, 657 cm^{-1}. Elem. Anal. calcd for $C_{60}H_{70}BF_{15}MoN_4Si$: C, 56.88; H, 5.57; N, 4.42. Found: C, 56.52; H, 5.29; N, 4.29.

Synthesis and characterization of ^{N}2b: In the glove box, [Mo(N){N(*t*Bu)(*m*-xyl)}$_3$] (^{N}**MoN**, 19.2 mg, 30.0 μmol, 1.00 equiv.), Ph_3SiH (7.8 mg, 30 μmol, 1.0 equiv.) and B(C_6F_5)$_3$ (15.4 mg, 30.0 μmol, 1.00 equiv.) were weighed in a screw-cap 4-mL vial. A magnetic stir bar was placed in the vial and 0.4 mL of C_6D_5Cl was added. After 5 min. of stirring, the clear yellow solution was transferred to a J-Young NMR tube. NMR analysis revealed the complete formation of ^{N}**2b** in a >95% spectroscopic yield. Back to the glove box, the C_6D_5Cl solution was filtered and evaporated to dryness, affording a brown oil. This residue was covered with toluene, and few drops of CH_2Cl_2 were added until the oil completely solubilized. The resulting solution was stored in the glove box's freezer (−40 °C) for a few days, affording yellow crystals of ^{N}**2b** (25 mg of a CH_2Cl_2/toluene solvate, 53% yield). ^{1}H NMR (400 MHz, Toluene-d_8) δ 7.90–7.83 (m, 6H), 7.36–7.31 (m, 9H), 6.68–6.65 (m, 3H), 4.32 (br s, *o*-H_{Xyl} + HB(C_6F_5)$_3$, 7H), 1.97 (br s, 18H), 0.97 (s, 27H). ^{11}B NMR (128 MHz, Toluene-d_8) δ −24.6 (d, J_{BH}=93.1). ^{19}F NMR (377 MHz, Toluene-d_8) δ −132.1 (d, J=20.7), −164.7 (t, J=20.5), −167.2 (ddd, J=24.3, 19.8, 7.1). IR (ATR) ν=2974, 2922, 2868, 1639, 1601, 1586, 1545, 1507, 1459, 1429, 1361, 1273, 1161, 1110, 1061, 1024, 965, 941, 891, 711, 697, 691 cm^{-1}. Elem. Anal. calcd for $C_{72}H_{70}BF_{15}MoN_4Si$•1 CH_2Cl_2•1 C_7H_8: C, 60.5; H, 5.08; N, 3.53. Found: C, 60.28; H, 5.08; N, 3.53.

Synthesis and characterization of ^{P}2a: In a glove box, [MoI(N){PhP($CH_2CH_2PCy_2$)$_2$}] (^{P}**MoN**, 10 mg, 12.5 μmol, 1.0 equiv.) was weighed in a screw-cap 4-mL vial. After addition of a magnetic stir bar, the solid was layered with a toluene-d_8 solution (0.5 mL) of B(C_6F_5)$_3$ (6.4 mg, 12.5 μmol, 1.0 equiv.). The vial was capped and stirred for a few minutes. Excess (ca. 3 equiv.) triethylsilane (Et_3SiH) was added to the resulting dark-red solution, which was then transferred to a J-Young NMR tube. NMR monitoring revealed completion of the reaction in 18 h. Back to the glove box, the solution was transferred to a round-bottom 10-mL screw-cap tube and concentrated to dryness, affording a dark purple oil. This was triturated with hexane (3×1.5 mL), causing a color change of the oil to brownish/red. Despite several attempts, it was not possible to obtain solid or crystalline material from this oil. The oil weighed 12 mg (66% yield). ^{1}H NMR (400 MHz, Toluene-d_8) δ 7.67 (t, J=10.8, 7.7, 2H), 7.21 (td, J=7.6, 2.2, 2H), 7.16–7.05 (m, 1H), 2.68 (s, 4H), 2.27–2.17 (m, 1H), 2.00 (d, J=12.7, 2H), 1.79 (dd, J=35.1, 11.8, 6H), 1.64 (s, 8H), 1.57–1.45 (m, 4H), 1.37 (d, J=15.0, 6H), 1.28–0.84 (m, 19H), 0.80 (t, J=7.6, 9H), 0.65 (q, J=7.5, 6H), 0.45 (s, 2H). ^{11}B NMR (128 MHz, Toluene-d_8) δ −24.5 (d, J=73.9). ^{19}F NMR (377 MHz, Toluene-d_8) δ −132.2 (d, J=22.7), −163.5 (t, J=20.6), −166.5 (t, J=18.9). ^{31}P{^{1}H} NMR (162 MHz, Toluene-d_8) δ 103.1 (1P), 67.1 (2P). IR (ATR) ν=2928, 2854, 1508, 1459, 1412, 1374, 1270, 1089, 1077, 1000, 964, 912, 890, 850, 812, 785, 739 cm^{-1}. Elem. Anal. calcd for $C_{58}H_{73}BF_{15}IMoNP_3Si$: C, 48.93; H, 5.17; N, 0.98. Found: C, 49.01; H, 5.34; N, 0.78.

Synthesis and characterization of ^{N}3: In the glove box, [Mo(N){N(*t*Bu)(*m*-xyl)}$_3$] (^{N}**MoN**, 38 mg, 60 μmol, 1.0 equiv.) and HB(C_6F_5)$_2$ (21 mg, 60 μmol, 1.0 equiv.) were weighed in a screw-cap 4-mL vial. The solids were dissolved in 2 mL of toluene. After hand-shaking to ensure complete solubilization of the reagents, the solution was concentrated to ~1 mL and pentane (4 mL) was added. The resulting solution was placed in the glove box's freezer (−40 °C) for a week, time during which amber crystals of ^{N}**3** grew, weighing 40 mg (68% yield). ^{1}H{^{11}B} NMR (400 MHz, C_6D_6) δ 6.61 (s, 3H), 6.13 (br s, 1H, B–H), 5.68 (br s, 6H), 1.95 (s, 18H), 1.24 (s, 27H). ^{11}B NMR (128 MHz, C_6D_6) δ −5.4. ^{19}F NMR (377 MHz, C_6D_6) δ −127.2 (d, J_{FF}=24, $4F_{ortho}$), −159.2 (t, J_{FF}=20, $2F_{para}$), −164.2 (dd, J_{FF}=20, 16, $4F_{meta}$). IR (ATR) ν=2974, 2931, 2863, 2417, 1640, 1601, 1587, 1511, 1465, 1458, 1392, 1381, 1361, 1278, 1168, 1148, 1087, 1062, 1055, 971, 954, 941, 891, 850, 760, 740, 732, 713, 691, 677. Elem. Anal. calcd for $C_{48}H_{55}BF_{10}MoN_4$: C, 58.55; H, 5.63; N, 5.69. Found: C, 59.72; H, 5.83; N, 5.51.

Synthesis and characterization of ^{P}3: In the glove box, [MoI(N){PhP($CH_2CH_2PCy_2$)$_2$}] (^{P}**MoN**, 7.8 mg, 9.8 μmol, 1.0 equiv.) and HB(C_6F_5)$_2$ (3.4 mg, 9.8 μmol, 1.0 equiv.) were weighed in a screw-cap 4-mL vial. The solids were dissolved in 0.5 mL of toluene-d_8 and the vial was hand-shaken to ensure complete solubilization of the reagents. The reaction mixture was transferred to J. Young NMR tube for NMR analysis, revealing the clean formation of [MoI{NB(H)(C_6F_5)$_2$}{PhP($CH_2CH_2PCy_2$)$_2$}] (^{P}**3**) in a >95% spectroscopic yield. Back to the glove box, the solution was transferred to a round-bottom 10-mL screw-cap tube and concentrated to dryness. The residue was then triturated in a few milliliters of pentane to give 16.3 mg of an amorphous solid (98% yield). ^{1}H{^{31}P} NMR (400 MHz, Toluene-d_8) δ 7.71 (dd, J=6.6, 3.0, 2H), 7.04–6.97 (m, 3H), 4.61 (br s, 1H), 2.68 (t, J=11.9, 2H), 2.33–2.22 (m, 4H), 2.14 (ddd, J=14.2, 5.6, 2.1, 2H), 1.96 (ddd, J=14.8, 4.9, 1.8, 2H), 1.88 (d, J=14.1, 4H), 1.82–1.70 (m, 4H), 1.70–1.48 (m, 9H), 1.33 (ddd, J=20.9, 13.6, 7.2, 8H), 1.23–0.83 (m, 13H), 0.74 (d, J=11.3, 2H), 0.61 (qd, J=12.1, 2.7, 2H). ^{11}B NMR (128 MHz, Toluene-d_8) δ −8.8. ^{19}F NMR (377 MHz, Toluene-d_8) δ=−130.5 (dd, J=24.7, 6.5), −161.3 (t, J=20.6), −165.2–−165.4 (m). ^{31}P{^{1}H} NMR (162 MHz, Toluene-d_8) δ 106.7 (1P), 60.2 (2P). IR (ATR) ν=2926, 2851, 1641, 1510 (s), 1462 (s), 1414, 1376, 1347, 1274 (m), 1200, 1177, 1085 (s), 1046 (m), 1002 (m), 966

(s), 914, 890, 849, 814, 741 (m), 692 (m). Elem. Anal. calcd.for $C_{46}H_{58}BF_{10}IMoNP_3$: C, 48.40; H, 5.12; N, 1.23. Found C, 48.11; H, 4.79; N, 1.02.

Crystallographic Details: Data for compounds ^{N}**1**, ^{N}**2b** and ^{N}**3** were collected at low temperature (100 K) on a Bruker Kappa Apex II diffractometer using a $Mo_{K\alpha}$ radiation ($\lambda = 0.71073$ Å) micro-source and equipped with an Oxford Cryosystems Cooler Device. The structures have been solved by Direct Methods and refined by means of least-squares procedures using the SHELXS97[28] program included in the software package WinGX version 1.63[29] or with the aid of the software package Crystal.[30] The Atomic Scattering Factors were taken from International tables for X-Ray Crystallography.[31] Hydrogen atoms were placed geometrically and refined using a riding model. All non-hydrogens atoms were anisotropically refined.

Deposition Number(s) 2218305 (for ^{N}**1**), 2218306 (for ^{N}**2b**) and 2218307 (for ^{N}**3**) contain(s) the supplementary crystallographic data for this paper. These data are provided free of charge by the joint Cambridge Crystallographic Data Centre and Fachinformationszentrum Karlsruhe Access Structures service.

DFT calculations: Geometry optimizations were performed using Gaussian 16 (Revision C01)[32] at the PBE0 level of hybrid density functional theory,[33] with inclusion of D3(bj) corrections in the optimization process.[34,35] The geometries of all located extrema are given as xyz coordinates data in a separate file (Geom.xyz) and in the Supporting Information (section IV.2). The atoms H, B, C, N, F, Si were represented by an svp basis set.[36] The Mo atom was represented by Dolg's pseudo potential and the associated basis set.[37,38] The solvent (benzene) influence was taken into consideration through single-point calculations on the gas-phase optimized geometries with SCRF calculations within the SMD model.[39] For the SCRF calculations, the atoms were treated with a def2-qzvp basis set.[40] All energies reported are Gibbs free energies obtained by summing the SMD energy (including D3 corrections) and the gas phase Gibbs contribution at 298 K and 1 atm.

Acknowledgements

A.C. is grateful to the French Ministry of National and Superior Education and Research (MENESR) for a Ph.D. fellowship. L.M. thanks Mitacs for a Globalink research fellowship. A.S., D.S. and Q.L.D. acknowledge the European Research Council (ERC) for funding (Grant Agreement 757501). All authors are indebted to the French National Center for Scientific Research (CNRS) for financial support. S.B. and N.M. acknowledge financial support from the Université de Toulouse.

Conflict of Interest

The authors declare no conflict of interest.

Data Availability Statement

The data that support the findings of this study are available in the supplementary material of this article.

Keywords: dinitrogen · frustrated Lewis pairs · molybdenum · nitrido complexes · silanes

[1] a) M. Appl, *Ullmanns Encycl. Ind. Chem.* **2011**, https://doi.org/10.1002/14356007.o02(((AMP)))lowbar(((SEMI)))o11; b) G. Ertl, *Angew. Chem. Int. Ed.* **2008**, *47*, 3524–3535; *Angew. Chem.* **2008**, *120*, 3578–3590; c) J. W. Erisman, M. A. Sutton, J. Galloway, Z. Klimont, W. Winiwarter, *Nat. Geosci.* **2008**, *1*, 636; d) R. Schlögl, *Angew. Chem. Int. Ed.* **2003**, *42*, 2004–2008; *Angew. Chem.* **2003**, *115*, 2050–2055; e) V. Smil, *Enriching the Earth: Fritz Haber, Carl Bosch, and the Transformation of World Food Production*, Mit Press, **2001**; f) V. Smil, *Nature* **1999**, *400*, 415; g) J. R. Jennings, *Catalytic Ammonia Synthesis: Fundamentals and Practice*, Springer, **1991**.

[2] a) S. Kim, F. Loose, P. J. Chirik, *Chem. Rev.* **2020**, *120*, 5637–5681; b) Z.-J. Lv, J. Wei, W.-X. Zhang, P. Chen, D. Deng, Z.-J. Shi, Z. Xi, *Natl. Sci. Rev.* **2020**, *7*, 1564–1583; c) A. Simonneau, *New J. Chem.* **2021**, *45*, 9294–9301.

[3] Y. Tanabe, Y. Nishibayashi, *Coord. Chem. Rev.* **2019**, *389*, 73–93.

[4] S. Bennaamane, M. F. Espada, A. Mulas, T. Personeni, N. Saffon-Merceron, M. Fustier-Boutignon, C. Bucher, N. Mézailles, *Angew. Chem. Int. Ed.* **2021**, *60*, 20210–20214; *Angew. Chem.* **2021**, *133*, 20372–20376.

[5] a) S. J. K. Forrest, B. Schluschaß, E. Y. Yuzik-Klimova, S. Schneider, *Chem. Rev.* **2021**, *121*, 6522–6587; b) I. Klopsch, E. Y. Yuzik-Klimova, S. Schneider, *Top. Organomet. Chem.* **2017**, *60*, 71–112.

[6] a) A. Simonneau, R. Turrel, L. Vendier, M. Etienne, *Angew. Chem. Int. Ed.* **2017**, *56*, 12268–12272; *Angew. Chem.* **2017**, *129*, 12436–12440; b) A. Coffinet, D. Specklin, L. Vendier, M. Etienne, A. Simonneau, *Chem. Eur. J.* **2019**, *25*, 14300–14303 ; c) A. Coffinet, D. Zhang, L. Vendier, S. Bontemps, A. Simonneau, *Dalton Trans.* **2021**, *50*, 5582–5589.

[7] a) *Frustrated Lewis Pairs* (Eds.: J. C. Slootweg, A. Jupp), Springer International Publishing, **2021**; b) D. W. Stephan, *Science* **2016**, *354*, 10.1126/science.aaf7229; c) D. W. Stephan, *Acc. Chem. Res.* **2015**, *48*, 306–316; d) D. W. Stephan, G. Erker, *Angew. Chem. Int. Ed.* **2015**, *54*, 6400–6441; *Angew. Chem.* **2015**, *127*, 6498–6541; e) D. W. Stephan, G. Erker, *Angew. Chem. Int. Ed.* **2010**, *49*, 46–76; *Angew. Chem.* **2010**, *122*, 50–81; f) G. Erker, D. W. Stephan, Eds., Frustrated Lewis Pairs II: Expanding the Scope, Springer-Verlag Berlin Heidelberg, **2013**; g) G. Erker, D. W. Stephan, Eds., Frustrated Lewis Pairs I: Uncovering and Understanding, Springer-Verlag Berlin Heidelberg, **2013**.

[8] a) Q. Liao, A. Cavaillé, N. Saffon-Merceron, N. Mézailles, *Angew. Chem. Int. Ed.* **2016**, *55*, 11212–11216; *Angew. Chem.* **2016**, *128*, 11378–11382; b) M. F. Espada, S. Bennaamane, Q. Liao, N. Saffon-Merceron, S. Massou, E. Clot, N. Nebra, M. Fustier-Boutignon, N. Mézailles, *Angew. Chem. Int. Ed.* **2018**, *57*, 12865–12868; *Angew. Chem.* **2018**, *130*, 13047–13050.

[9] a) N. S. Lambic, R. D. Sommer, E. A. Ison, *J. Am. Chem. Soc.* **2016**, *138*, 4832–4842; b) N. S. Lambic, R. D. Sommer, E. A. Ison, *ACS Catal.* **2017**, *7*, 1170–1180; c) C. A. Brown, M. Abrahamse, E. A. Ison, *Dalton Trans.* **2020**, *49*, 11403–11411.

[10] N. Zwettler, S. P. Walg, F. Belaj, N. C. Mösch-Zanetti, *Chem. Eur. J.* **2018**, *24*, 7149–7160.

[11] N. Zwettler, N. C. Mösch-Zanetti, *Chem. Eur. J.* **2019**, *25*, 6064–6076.

[12] L. Chatelain, E. Louyriac, I. Douair, E. Lu, F. Tuna, A. J. Wooles, B. M. Gardner, L. Maron, S. T. Liddle, *Nat. Commun.* **2020**, *11*, 337.

[13] a) C. E. Laplaza, C. C. Cummins, *Science* **1995**, *268*, 861–863 ; b) C. E. Laplaza, M. J. A. Johnson, J. C. Peters, A. L. Odom, E. Kim, C. C. Cummins, G. N. George, I. J. Pickering, *J. Am. Chem. Soc.* **1996**, *118*, 8623–8638; c) J. J. Curley, T. R. Cook, S. Y. Reece, P. Müller, C. C. Cummins, *J. Am. Chem. Soc.* **2008**, *130*, 9394–9405.

[14] Q. Liao, N. Saffon-Merceron, N. Mézailles, *ACS Catal.* **2015**, *5*, 6902–6906.

[15] E. L. Sceats, J. S. Figueroa, C. C. Cummins, N. M. Loening, P. Van der Wel, R. G. Griffin, *Polyhedron* **2004**, *23*, 2751–2768.

[16] L. A. Wickramasinghe, T. Ogawa, R. R. Schrock, P. Müller, *J. Am. Chem. Soc.* **2017**, *139*, 9132–9135.

[17] Y. Liu, T.-C. Lau, *J. Am. Chem. Soc.* **2019**, *141*, 3755–3766.

[18] A. R. Jupp, T. C. Johnstone, D. W. Stephan, *Inorg. Chem.* **2018**, *57*, 14764–14771.

[19] Si–H bond splitting promoted by FLP: a) M. Alcarazo, C. Gomez, S. Holle, R. Goddard, *Angew. Chem. Int. Ed.* **2010**, *49*, 5788–5791; *Angew. Chem.* **2010**, *122*, 5924–5927; b) D. Chen, V. Leich, F. Pan, J. Klankermayer, *Chem. Eur. J.* **2012**, *18*, 5184–5187; c) W. Nie, H. F. T. Klare, M. Oestreich, R. Fröhlich, G. Kehr, G. Erker, *Z. Naturforsch. B* **2012**, *67*, 987–994; d) S. Tamke, C.-G. Daniliuc, J. Paradies, *Org. Biomol. Chem.* **2014**, *12*, 9139–9144; e) A. Gudz, P. R. Payne, M. R. Gagné, *Organometallics* **2017**, *36*, 4047–4053; f) I. Avigdori, A. Pogoreltsev, A. Kaushanski, N. Fridman, M.

Gandelman, *Angew. Chem. Int. Ed.* **2020**, *59*, 23476–23479; *Angew. Chem.* **2020**, *132*, 23682–23685; g) C. A. Brown, M. Abrahamse, E. A. Ison, *Dalton Trans.* **2020**, *49*, 11403–11411; h) I. Zulkifly, A. V. Protchenko, M. Á. Fuentes, J. Hicks, S. Aldridge, *Z. Anorg. Allg. Chem.* **2022**, *648*, e202200110.
[20] B–H bond splitting promoted by FLP: a) M. A. Dureen, A. Lough, T. M. Gilbert, D. W. Stephan, *Chem. Commun.* **2008**, 4303–4305; b) P. Eisenberger, A. M. Bailey, C. M. Crudden, *J. Am. Chem. Soc.* **2012**, *134*, 17384–17387; c) C. Appelt, J. C. Slootweg, K. Lammertsma, W. Uhl, *Angew. Chem. Int. Ed.* **2013**, *52*, 4256–4259; *Angew. Chem.* **2013**, *125*, 4350–4353; d) J. Zheng, Y. Wang, Z. H. Li, H. Wang, *Chem. Commun.* **2015**, *51*, 5505–5508; e) X. Fan, J. Zheng, Z. H. Li, H. Wang, *J. Am. Chem. Soc.* **2015**, *137*, 4916–4919; f) Q. Yin, H. F. T. Klare, M. Oestreich, *Angew. Chem. Int. Ed.* **2017**, *56*, 3712–3717; *Angew. Chem.* **2017**, *129*, 3766–3771; g) Y.-C. Lin, E. Hatzakis, S. M. McCarthy, K. D. Reichl, T.-Y. Lai, H. P. Yennawar, A. T. Radosevich, *J. Am. Chem. Soc.* **2017**, *139*, 6008–6016; h) Y. Pan, J. Cui, Y. Wei, Z. Xu, T. Wang, *Dalton Trans.* **2021**, *50*, 8947–8954; i) L. J. Bole, M. Uzelac, A. Hernán-Gómez, A. R. Kennedy, C. T. O'Hara, E. Hevia, *Inorg. Chem.* **2021**, *60*, 13784–13796.
[21] Z. M. Heiden, L. A. Paige, *Organometallics* **2015**, *34*, 1818–1827.
[22] S. Ilic, A. Alherz, C. B. Musgrave, K. D. Glusac, *Chem. Soc. Rev.* **2018**, *47*, 2809–2836.
[23] a) D. J. Parks, W. E. Piers, *J. Am. Chem. Soc.* **1996**, *118*, 9440–9441; b) D. J. Parks, J. M. Blackwell, W. E. Piers, *J. Org. Chem.* **2000**, *65*, 3090–3098; c) S. Rendler, M. Oestreich, *Angew. Chem. Int. Ed.* **2008**, *47*, 5997–6000; *Angew. Chem.* **2008**, *120*, 6086–6089; d) K. Sakata, Hiroshi. Fujimoto, *J. Org. Chem.* **2013**, *78*, 12505–12512; e) A. Y. Houghton, J. Hurmalainen, A. Mansikkamäki, W. E. Piers, H. M. Tuononen, *Nat. Chem.* **2014**, *6*, 983–988.
[24] J. J. Curley, E. L. Sceats, C. C. Cummins, *J. Am. Chem. Soc.* **2006**, *128*, 14036–14037.
[25] C. Wang, G. Erker, G. Kehr, K. Wedeking, R. Fröhlich, *Organometallics* **2005**, *24*, 4760–4773.
[26] D. J. Parks, R. E. von H. Spence, W. E. Piers, *Angew. Chem. Int. Ed. Engl.* **1995**, *34*, 809–811.
[27] R. K. Harris, E. D. Becker, S. M. Cabral de Menezes, P. Granger, R. E. Hoffman, K. W. Zilm, *Pure Appl. Chem.* **2008**, *80*, 59–84.
[28] SHELX97 [Includes SHELXS97, SHELXL97, CIFTAB] – Programs for Crystal Structure Analysis (Release 97–2). G. M. Sheldrick, Institüt für Anorganische Chemie der Universität, Tammanstrasse 4, D-3400 Göttingen, Germany, 1998.
[29] L. J. Farrugia, *J. Appl. Crystallogr.* **1999**, *32*, 837–838.
[30] P. W. Betteridge, J. R. Carruthers, R. I. Cooper, K. Prout, D. J. Watkin, *J. Appl. Crystallogr.* **2003**, *36*, 1487–1487.
[31] International Tables for X-Ray Crystallography Vol. IV, Kynoch press, Birmingham, England, **1974**.
[32] M. J. Frisch, G. W. Trucks, H. B. Schlegel, G. E. Scuseria, M. A. Robb, J. R. Cheeseman, G. Scalmani, V. Barone, G. A. Petersson, H. Nakatsuji, X. Li, M. Caricato, A. V. Marenich, J. Bloino, B. G. Janesko, R. Gomperts, B. Mennucci, H. P. Hratchian, J. V. Ortiz, A. F. Izmaylov, J. L. Sonnenberg, D. Williams-Young, F. Ding, F. Lipparini, F. Egidi, J. Goings, B. Peng, A. Petrone, T. Henderson, D. Ranasinghe, V. G. Zakrzewski, J. Gao, N. Rega, G. Zheng, W. Liang, M. Hada, M. Ehara, K. Toyota, R. Fukuda, J. Hasegawa, M. Ishida, T. Nakajima, Y. Honda, O. Kitao, H. Nakai, T. Vreven, K. Throssell, J. Montgomery, J. A., J. E. Peralta, F. Ogliaro, M. J. Bearpark, J. J. Heyd, E. N. Brothers, K. N. Kudin, V. N. Staroverov, T. A. Keith, R. Kobayashi, J. Normand, K. Raghavachari, A. P. Rendell, J. C. Burant, S. S. Iyengar, J. Tomasi, M. Cossi, J. M. Millam, M. Klene, C. Adamo, R. Cammi, J. W. Ochterski, R. L. Martin, K. Morokuma, O. Farkas, J. B. Foresman, D. J. Fox, **2016**.
[33] C. Adamo, V. Barone, *J. Chem. Phys.* **1999**, *110*, 6158–6170.
[34] S. Grimme, J. Antony, S. Ehrlich, H. Krieg, *J. Chem. Phys.* **2010**, *132*, 10.1063/1.3382344.
[35] S. Grimme, S. Ehrlich, L. Goerigk, *J. Comput. Chem.* **2011**, *32*, 1456–1465.
[36] A. Schäfer, H. Horn, R. Ahlrichs, *J. Chem. Phys.* **1992**, *97*, 2571–2577.
[37] D. Andrae, U. Häußermann, M. Dolg, H. Stoll, H. Preuß, *Theor. Chim. Acta* **1990**, *77*, 123–141.
[38] K. A. Peterson, D. Figgen, E. Goll, H. Stoll, M. Dolg, *J. Chem. Phys.* **2003**, *119*, 11113–11123.
[39] A. V. Marenich, C. J. Cramer, D. G. Truhlar, *J. Phys. Chem. B* **2009**, *113*, 6378–6396.
[40] F. Weigend, R. Ahlrichs, *Phys. Chem. Chem. Phys.* **2005**, *7*, 3297–3305.

Manuscript received: December 2, 2022
Accepted manuscript online: February 20, 2023
Version of record online: March 24, 2023